Uzbekistan Journal of Polymers

journal homepage: https://uzpolymerjournal.com/
ISSN (online): 2181-3256 (print) 2181-3246

DFT INVESTIGATION OF BAND GAP MODULATION BY SUBSTITUTIONAL IMPURITY DEFECTS IN ABX_3 PEROVSKITES

Khamzaev A., Marasulov M.B., Nurgaliev I.N.

Institute of Polymer Chemistry and Physics Uzbekistan Academy of Sciences, 100128, Tashkent, Uzbekistan

ARTICLE INFO

Received: 11 March 2025
Revised: 01 July 2025
Accepted: 07 July 2025

Keywords:
halide perovskites, DFT calculations, cation substitution, band gap modulation, ionic mobility, structural stability.

Corresponding author: Nurgaliev I.
ilnarvodnik@gmail.com

ABSTRACT

In this study, density functional theory (DFT) calculations were employed to investigate the structural and electronic properties of mixed halide perovskites with the general formula ABX_3, where partial substitution of the A-site methylammonium (MA^+) cation was performed using NH_4^+, $(NH_2)_2CH^+$ (formamidinium, FA^+), and Cs^+. The impact of these substitutions on lattice parameters, band gap energies, and ionic mobility was systematically analyzed. The results revealed that partial cation substitution introduces notable lattice distortions and modulates the band gap of the perovskite structures. A correlation was established between the ionic radius of the substituting cation and the reduction in band gap energy, with larger cations contributing to narrower band gaps. Moreover, the incorporation of rigid and dipolar cations was found to suppress ion migration, potentially enhancing the long-term stability of perovskite materials. The findings suggest that targeted cation engineering in halide perovskites can serve as an effective strategy for optimizing both electronic properties and operational durability, opening pathways for the design of high-performance, stable perovskite solar cells.

Introduction

Halide perovskite solar cells have emerged as highly promising candidates for large-scale photovoltaic applications, owing to their exceptional power conversion efficiencies (currently reaching a record value of 26.7% for a single-junction device) [1] and relatively straightforward fabrication processes. Nevertheless, the widespread commercialization of these materials remains constrained by their pronounced operational instability under real-world environmental conditions [2,3]. At the atomic scale, intrinsic lattice defects in perovskite structures act as nucleation centers for degradation phenomena by promoting ionic migration [4–6], facilitating parasitic chemical reactions [7,8], inducing structural phase transitions [9,10], and driving phase segregation processes [11].

Given the inherent complexities and limitations of experimental techniques for probing the atomic-scale structure of defects, the predominant insights into the defect physics of halide perovskites have been obtained from first-principles electronic structure calculations within the framework of density functional theory (DFT) [11-17]. In accordance with established paradigms in semiconductor defect chemistry, research efforts have primarily focused on fundamental point defects, including vacancies, interstitial species, and antisite substitutions. A key finding consistently reported across these computational studies is that, under thermodynamic equilibrium growth conditions, the dominant point defects in these materials are characterized by shallow electronic levels, thereby minimally perturbing the optoelectronic properties of the host perovskite lattice.

Despite the predominance of shallow-level point defects under equilibrium conditions, their presence is not benign, as they can significantly influence ion transport dynamics, enhance non-radiative recombination pathways, and catalyze the formation of more complex defect aggregates under operational stress. Furthermore, under realistic device conditions—such as illumination, electric fields, and thermal gradients—the population and distribution of defects may deviate from equilibrium predictions, leading to dynamic defect formation and annihilation processes that exacerbate long-term instability.

In particular, the migration of mobile ionic species, often initiated at vacancy sites, contributes to field-induced ion redistribution, which is directly linked to current–voltage hysteresis and transient performance losses in perovskite solar cells [18, 19]. Concurrently, defect-assisted chemical reactions at grain boundaries and interfaces, driven by external stimuli, accelerate the degradation of both the perovskite absorber and adjacent charge transport layers [20]. Additionally, localized structural instabilities can trigger phase transitions from the photoactive perovskite phase to non-perovskite polymorphs [21], while compositional inhomogeneities arising from phase segregation further deteriorate device stability and efficiency [22].

To systematically address these challenges, a comprehensive understanding of defect thermodynamics, migration kinetics, and their coupling to external perturbations is imperative. Advanced DFT-based methodologies, incorporating hybrid functionals, spin–orbit coupling, and finite-temperature effects, are increasingly employed to provide accurate defect formation energies, charge transition levels, and migration barriers. These computational insights are essential not only for identifying defect-tolerant perovskite compositions but also for guiding targeted defect passivation strategies, optimized synthesis protocols, and the design of robust device architectures that mitigate the detrimental impact of defect-related phenomena.

The complete substitution of Pb^{2+} with Sn^{2+} in halide perovskites has already been successfully demonstrated; however, the stability of such compounds remains a significant challenge [23]. Additionally, both theoretical and experimental studies have investigated the partial replacement of Pb^{2+} with Sn^{2+} and Sr^{2+} in various perovskite systems, including those based on Ca^{2+}, Cd^{2+}, Bi–Ti, and chalcogenide perovskites. In [24] performed computational screening of isovalent lead substitutions, identifying Mg as a promising candidate for partial Pb replacement. Their results revealed that the bandgap can be tuned by approximately 0.8 eV through variation of the A-site cation radius in the ABO_3-type perovskite structure. The incorporating a mixture of guanidinium ($HNCHNH_3^+$) and methylammonium (MA) at the A-site of $APbI_3$ leads to an enhancement in short-circuit current. These studies demonstrate that the combination of metal cations and organic cations introduces substantial structural and electronic diversity, offering a versatile approach for tailoring the properties of halide perovskites.

Enhancing the stability of halide perovskites is a critical objective for the further development of this research field. In the context of perovskite solar cell stability, understanding the origins of current–voltage hysteresis is of particular importance. Haruyama et al. conducted theoretical investigations of ion diffusion barriers for both cations and anions in tetragonal $CH_3NH_3PbI_3$ and trigonal $(NH_2)_2CHPbI_3$ phases [25]. Their calculations indicated that ion displacement could explain the hysteresis observed in current–voltage characteristics, and that suppressing ion diffusion would likely improve device stability. Despite the remarkable progress in perovskite research, the detailed mechanisms underlying degradation and long-term stability remain insufficiently understood, posing a major obstacle to commercialization and large-scale application.

To gain deeper insights into the durability of ABX_3 organic–halide perovskites, we carried out theoretical investigations on the statistical and dynamic properties of partially substituted halide perovskites in which methylammonium (MA) cations are partially replaced with NH_4^+, $(NH_2)_2CH^+$, or Cs^+ (hereafter referred to as X). This work focuses primarily on the suppression of organic cation diffusion through partial substitution. Figure 1 presents a schematic illustration of possible defect states, explaining the mechanism of reduced A-site cation (MA or X) mobility in perovskite structures with partial cation substitution.

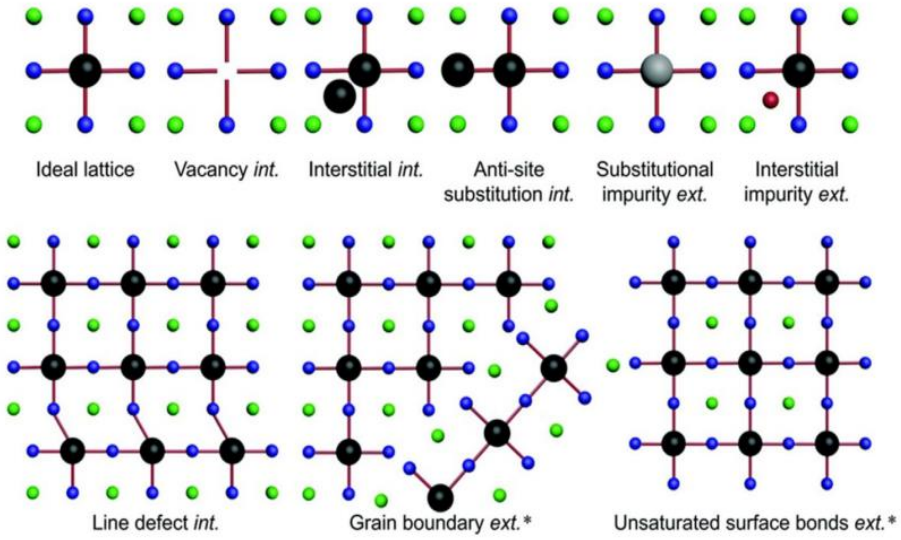

Figure 1. *Schematic representation of the ideal perovskite lattice with the formula ABX_3 and possible defects within the structure (green, black, and blue dots represent the A-, B-, and X-sites, respectively; red and gray dots indicate impurity atoms).*

Computational Study

First-principles calculations based on density functional theory (DFT) were performed to investigate the electronic properties, specifically the band gap, of a series of halide perovskites with the general formula ABX_3. Here, A represents various organic cations including methylammonium (MA^+), formamidinium (FA^+), ammonium (NH_4^+), and guanidinium (GUA^+), while X denotes halide anions such as I^-, Br^-, and Cl^-. The central focus was to systematically evaluate the effect of the B-site cation (Ge^{2+}, Pb^{2+}, Zn^{2+}, Mg^{2+}, Sn^{2+}) and A-site organic cation substitutions on the band gap tuning in these perovskite frameworks.

The structural optimizations and electronic structure calculations were carried out using the Vienna Ab initio Simulation Package (VASP). Projector augmented-wave (PAW) pseudopotentials were employed, and the exchange-correlation interaction was treated within the generalized gradient approximation (GGA) using the Perdew–Burke–Ernzerhof (PBE) functional. To account for the known underestimation of band gaps in GGA calculations, additional hybrid functional calculations using the Heyd–Scuseria–Ernzerhof (HSE06) functional were performed for selected compositions. Spin–orbit coupling (SOC) effects were included for Pb- and Sn-based perovskites due to their significant influence on the electronic structure.

All structures were fully relaxed until the forces on each atom were less than 0.01 eV/Å, and the total energy convergence criterion was set to 10^{-5} eV. A Monkhorst–Pack k-point mesh of 5×5×5 was used for Brillouin zone sampling in the cubic perovskite phases. The cutoff energy for the plane-wave basis set was fixed at 500 eV.

The calculated band gaps were analyzed in relation to the ionic radius and electronegativity of the B-site metal cations, as well as the steric effects and dipole moments of the organic A-site cations. Correlations between the structural distortions induced by different cation combinations and the resulting band gap values were established. The obtained results provide insights into the compositional engineering of halide perovskites for optoelectronic applications, highlighting potential lead-free alternatives with optimized electronic properties.

Results and Discussion

When incorporating organic cations with different ionic radii into the perovskite structure, distortions of the crystal lattice are observed. These distortions arise due to both the size mismatch of the cations and the differences in interactions between the A-site cations and the surrounding perovskite framework. The introduction of larger cations can restrict the migration of smaller cations by narrowing migration pathways and increasing energy barriers, while the diffusion of larger cations is also hindered by local lattice distortions and enhanced structural rigidity.

In this study, we investigate the effect of partial substitution of $CH_3NH_3^+$ (methylammonium, MA^+) cations in perovskites based on $CH_3NH_3PbI_3$, $CH_3NH_3SnI_3$, and mixed $CH_3NH_3Pb(Sn)I_3$ systems on the band gap, lattice parameters, and cation diffusion properties. The obtained results provide insights into the potential of compositional engineering to design stable perovskite solar cells with improved durability (Fig. 2).

Our calculations show that partial substitution of MA^+ with alternative organic cations, such as NH_4^+ or $(NH_2)_2CH^+$, leads to noticeable changes in the structural parameters of the perovskite lattice. The organic cations contribute minimally to the frontier electronic states but may indirectly affect the band structure through induced lattice distortions and electrostatic interaction. This compaction of the lattice contributes to enhanced structural stability, potentially mitigating ion migration pathways that are commonly associated with long-term material degradation.

Additionally, the calculated band gaps of the substituted systems exhibit moderate variations compared to the pristine structures. The mixed $CH_3NH_3Pb(Sn)I_3$ (1.61 eV) composition, in particular, demonstrates a reduced band gap, which may improve light absorption in the visible spectrum, thereby enhancing photovoltaic performance. These findings are in agreement with previous experimental observations and theoretical predictions indicating that cation substitution can serve as an effective tool for fine-tuning the electronic properties of halide perovskites.

Moreover, the analysis of cation diffusion barriers reveals that the incorporation of larger or more rigid cations reduces the mobility of A-site species within the lattice. This suppression of ionic migration is crucial for improving operational stability and minimizing hysteresis effects in current-voltage characteristics.

Structural and electronic property calculations were performed for systems in which half of the MA^+ cations in the unit cell were partially substituted with NH_4^+ or $(NH_2)_2CH^+$ (formamidinium, FA^+). The calculated parameters, including the Goldschmidt tolerance factor ttt and ionic radii of the cations, are presented in Table 1. Analysis of the ttt values indicates that the proposed cation combinations are compatible with stable perovskite structure formation, although deviations of ttt from the ideal value of 1 suggest the possibility of local lattice distortions. The coexistence of two types of cations with different ttt values at the A-site is expected to induce further structural modifications while preserving the overall perovskite framework.

To evaluate the influence of dispersion interactions, additional calculations were performed using the Tkatchenko–Scheffler (TS) correction scheme. According to Table 1, the lattice parameters of the optimized supercell without dispersion corrections were a = 12.87 Å, b = 12.88 Å, c = 13.03 Å with a volume of 2149 Å^3. Upon inclusion of dispersion corrections, the optimized lattice parameters were a = 12.66 Å, b = 12.68 Å, and c = 12.82 Å with a volume of 2057 Å^3. Accounting for dispersion interactions results in a more compact structure and brings the lattice parameters closer to those characteristic of the cubic perovskite phase.

The calculated band gap, including dispersion corrections, showed good agreement with the experimental value of approximately 1.55 eV [26]. The improvement in band gap estimation upon inclusion of dispersion corrections has been previously discussed in [89], where similar trends were

reported. Therefore, to increase the accuracy of electronic structure and band gap calculations in such systems, it is essential to include dispersion interactions, which significantly affect both the lattice geometry and its electronic properties.

Table 1

Optimized structural parameters of partially substituted $MAPbI_3$ calculated using DFT with dispersion correction.

$MA_{0.5}X_{0.5}PbI_3$	Band gap, eV
$X = NH_4^+$	1,35
$X = (NH_2)_2CH^+$	1,35
$X = Cs^+$	1,53

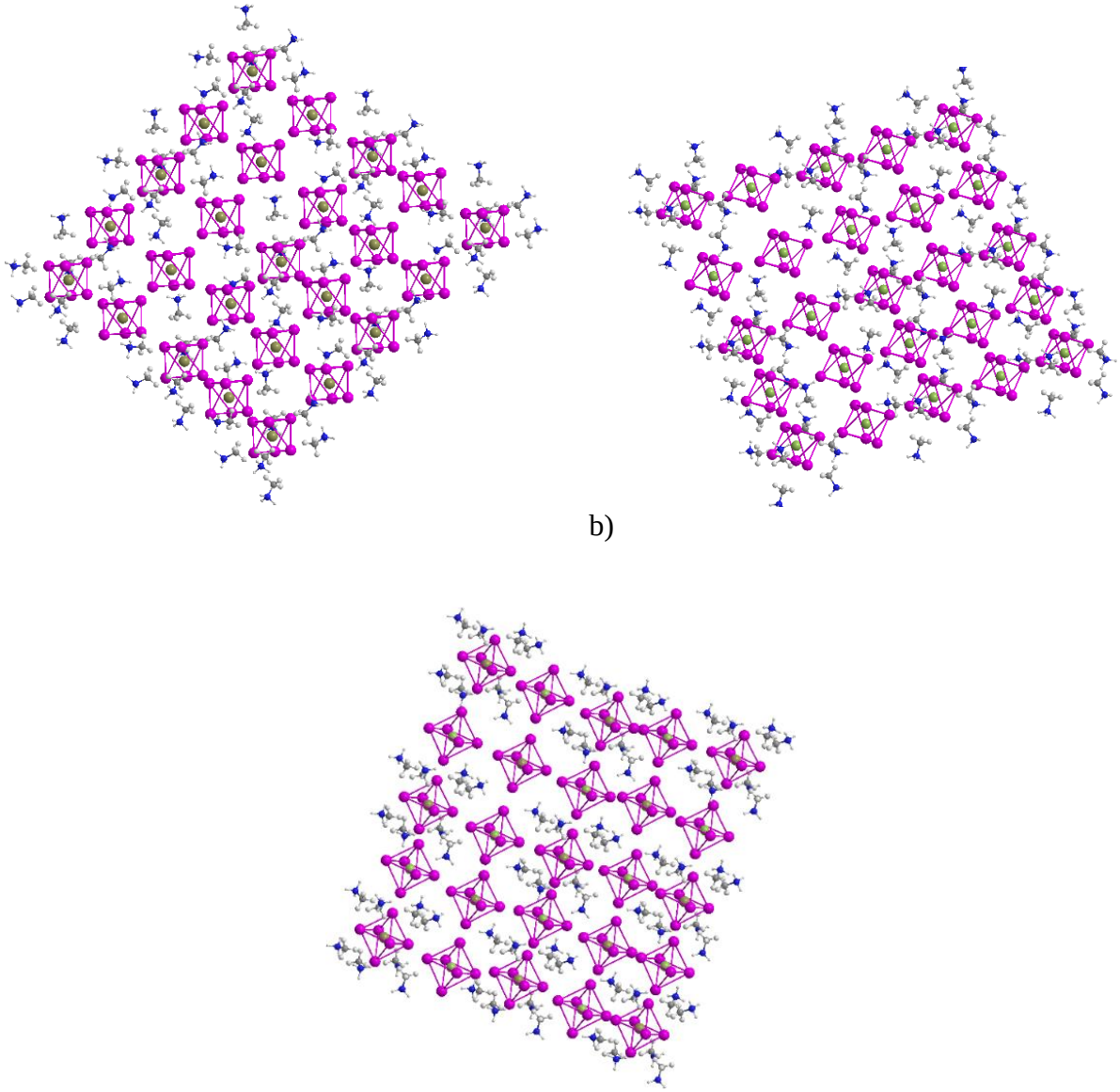

a) b)

c)

Figure 2. *Structural models of $CH_3NH_3PbI_3$, $CH_3NH_3SnI_3$, and $CH_3NH_3Pb(Sn)I_3$.*

We partially substituted the organic cation ($CH_3NH_3^+$, MA^+) with other cations, namely NH_4^+, $(NH_2)_2CH^+$, and Cs^+. In all cases, four MA^+ ions were replaced by substituent cations within a supercell while the remaining four MA^+ cations retained their original positions. The substitutions were introduced in the ab-plane to create an ordered distribution, as this planar arrangement induces stronger structural distortions compared to random substitution.

The unit cell volumes of the substituted perovskites vary compared to the pristine $MAPbI_3$. Generally, the cell volume increases with the ionic radius of the substituent organic cation. However, in the case of the inorganic Cs^+ it is a rigid spherical cation without a dipole, unlike organic ions with the perovskite framework compared to those of organic cations.

The lattice angles of the partially substituted perovskites slightly deviate from those of the unsubstituted $MAPbI_3$ structure. Among the studied systems, the $((NH_2)_2CH^+)_{0.5}MA_{0.5}PbI_3$ structure exhibits the most pronounced distortion, which correlates with the fact that the ionic radius of the $(NH_2)_2CH^+$ cation is the largest among the considered A-site cations. These results indicate that partial substitution in lead halide perovskites can effectively modify the internal volume of the perovskite framework, influencing ion mobility within the A-site.

Fig. 3 (a) shows the partial density of states (PDOS) of $MAPbI_3$. The PDOS analysis reveals that the valence band maximum is primarily derived from I 5p orbitals, while the conduction band minimum originates from Pb 6p orbitals, which is consistent with previous reports [27]. Fig. 3 (b–d) present the PDOS of the partially substituted perovskites. These figures demonstrate that the overall electronic structures of the substituted perovskites remain similar to that of pristine $MAPbI_3$. As reported in earlier studies [91–95], the A-site organic cation typically stabilizes the crystal structure but has minimal contribution to the frontier electronic states near the band edges. This observation is confirmed in our study of partially substituted $MAPbI_3$ perovskites.

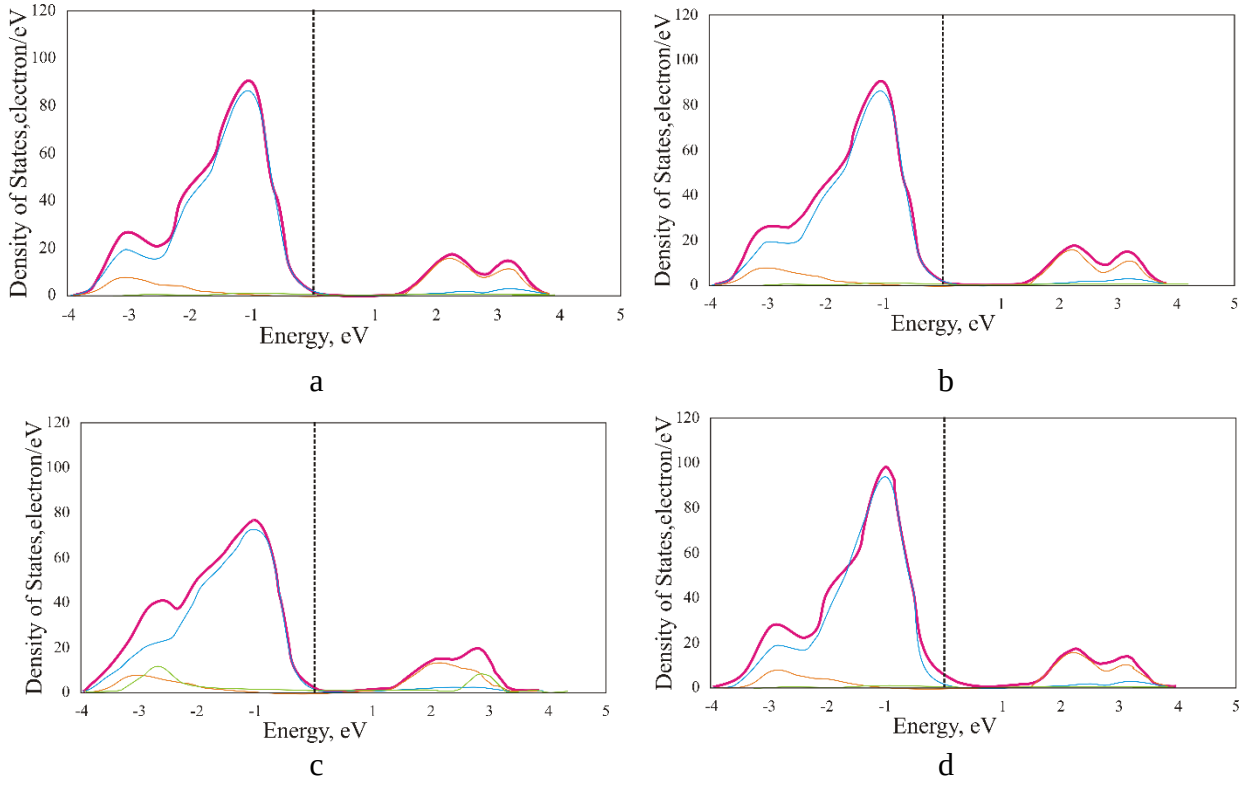

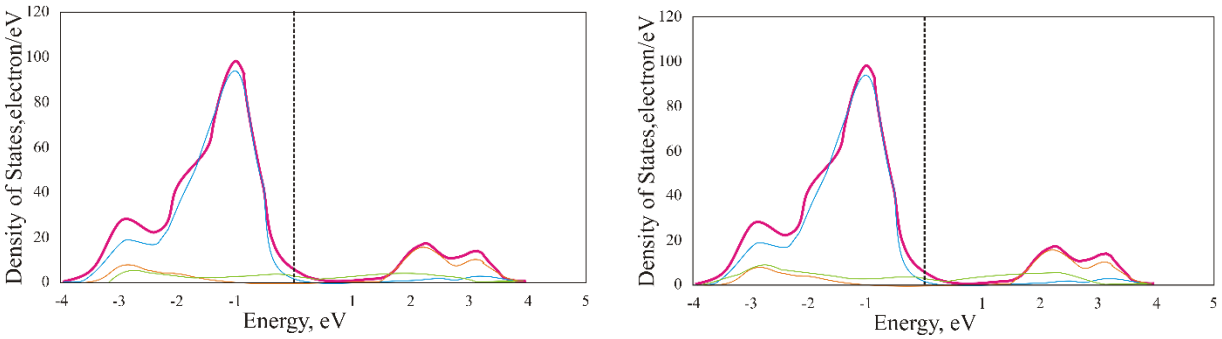

Figure 3. *Calculated partial density of states (PDOS) of (a) $CH_3NH_3PbI_3$, partially substituted $MAPbI_3$ by: (b) $(NH_2)_2CH^+$, (c) $(CH_3)_2NH_2^+$ (d) Cs^+, (e) $CH_3CH_2NH_3^+$, (f) $NH_2NH_3^+$. Where: blue - total, black - I 5p, yellow - Pb 6p, green - organic cation*

Table 2

Calculated band gap and HOMO-LUMO gap values of the electronic structures of mixed perovskites and organic cations

Perovskite	Band gap, eV	Cation	HOMO-LUMO gap of isolated cation molecule, eV
$CH_3NH_3ZnI_3$	0.667	$(CH_2)_3NH_2^+$	6.565
$CH_3NH_3GeI_3$	1.549	$(CH_3)_2NH_2^+$	6.3086
$CH_3NH_3PbI_3(Cl)$	1.444	$(CH_3)_3NH^+$	6.3396
$CH_3NH_3PbI_3(Br)$	1.396	$(CH_3)_4N^+$	6.3498
NH_2CHNH_2Pb	0.754	$(NH_2)_2CH^+$	6.6961
NH_2CHNH_2Ge	0.736	$C(NH_2)_3^+$	7.4204
NH_2CHNH_2Mg	0.74	$C_3N_2H_5^+$	6.4821
NH_2CHNH_2Sn	0.725	$C_4H_{12}N_2^+$	6.4037
NH_2CHNH_2Zn	0.73	$CH_3CH_2NH_3^+$	6.3346
		$CH_3NH_3^+$	9.2492
		$N(C_3H_7)_4^+$	6.4347
		$NH_2NH_3^+$	6.2594

Nevertheless, the calculated band gaps of the partially substituted perovskites and HOMO-LUMO gap of isolated cation molecule, summarized in Table 2, are slightly smaller than that of pristine $MAPbI_3$. Additionally, we performed electronic structure calculations on mixed perovskites containing various organic cations and different divalent metal cations (Ge^{2+}, Pb^{2+}, Zn^{2+}, Mg^{2+}, Sn^{2+}) combined with halide anions (Br^- or Cl^-). $CH_3NH_3GeI_3$ and $CH_3NH_3PbI_3(Cl)$ show moderate band gaps of **1.549 eV** and **1.444 eV**, respectively, while halide substitution (Cl^- and Br^-) in $CH_3NH_3PbI_3$ slightly reduces the band gap compared to the pristine structure, aligning with previous observations that halide composition modulates the electronic properties.

Regarding formamidinium ($NH_2CHNH_2^+$)-based perovskites, relatively narrow band gaps between **0.725 eV** and **0.754 eV** are observed, regardless of the B-site metal (Pb^{2+}, Ge^{2+}, Sn^{2+}, Zn^{2+}, Mg^{2+}). This suggests that the incorporation of the formamidinium cation generally stabilizes lower band gap values, which may be beneficial for enhancing light absorption in photovoltaic applications.

For the isolated organic cations, the calculated HOMO-LUMO gaps are substantially larger, ranging from **6.2594 eV** for $NH_2NH_3^+$ to **9.2492 eV** for $CH_3NH_3^+$. These values confirm that the

organic cations do not directly contribute to the frontier electronic states (valence band maximum and conduction band minimum), as their electronic levels are located far from the perovskite's band edges. This supports the widely accepted understanding that the A-site cations primarily stabilize the lattice structure and modulate the tolerance factor, rather than significantly altering the band gap.

Interestingly, cations such as $C(NH_2)_3^+$ and $(NH_2)_2CH^+$ exhibit slightly higher HOMO-LUMO gap s(**7.4204 eV** and **6.6961 eV**, respectively) compared to other organic species, which may relate to their larger size and specific electronic configurations.

According to the calculated electronic properties of mixed perovskites and various organic cations (Table 2), it is possible to control the band gap through compositional tuning. A correlation is observed between the ionic radius of the substituting cation and HOMO-LUMO gap reduction, likely due to induced structural distortions and electronic environment modifications. Additionally, the study demonstrates the ability to modulate donor and acceptor levels through the incorporation of specific dopant cations, thereby allowing for targeted adjustment of the band gap and electronic properties of mixed perovskites. This strategy opens new prospects for the purposeful design of perovskite materials with tailored electronic characteristics.

A computational investigation of the structural and electronic properties of partially substituted cubic perovskites with the composition $MA_{0.5}X_{0.5}PbI_3$ (where X = NH_4^+, $(NH_2)_2CH^+$, and Cs^+) was carried out using density functional theory (DFT). The electronic structure analysis revealed that the band gap of all partially substituted perovskites is slightly reduced compared to pristine $MAPbI_3$.

The findings also suggest the possibility of controlling defect states and trap densities in wide-bandgap perovskites through cation engineering. This can be achieved by incorporating dipolar cations and optimizing their orientation within the lattice, effectively enhancing defect tolerance.

Overall, this study demonstrates that partial substitution of the organic cation with larger cations can suppress ion migration at the A-site and potentially improve the long-term stability of halide perovskite-based solar cells.

Conclusions

This work demonstrates the potential of partial A-site cation substitution in halide perovskites as an effective approach to tune structural and electronic properties. DFT calculations revealed that replacing methylammonium (MA^+) with NH_4^+, $(NH_2)_2CH^+$, and Cs^+ leads to moderate lattice distortions, reduced band gap energies, and decreased ionic mobility, all of which contribute to enhanced material stability. A clear relationship was observed between the size of the substituting cation and the reduction in the band gap, indicating that larger cations induce more significant electronic modifications.

Additionally, the study confirmed that organic cations, while structurally stabilizing the perovskite lattice, have minimal direct impact on the frontier electronic states. However, through compositional tuning, it is possible to influence defect formation, carrier dynamics, and ultimately the optoelectronic performance of perovskite solar cells.

Overall, the findings highlight that cation engineering, particularly through partial substitution strategies, is a promising route to design halide perovskite materials with optimized band gaps and improved resistance to ion migration. This approach provides new opportunities for the development of durable, high-efficiency perovskite-based photovoltaic devices suitable for long-term practical applications.

REFERENCES

[1]. Nayak M., Akhtar A.J., Saha S.K. Theoretical estimation to double the performance of perovskite solar cells using a graded absorber layer. Sustainable Energy Fuels. 2025, 9, 1305-1316. https://doi.org/10.1039/D4SE01271B

[2]. Md.H. Miah, Md.B. Rahman, M. Nur-E-Alam, M.A. Islam, M. Shahinuzzaman, Md.R Rahman, Md.H, Ullahi, M.U. Khandaker Key degradation mechanisms of perovskite solar cells and strategies for enhanced stability: issues and prospects. RSC Adv., 2025, 15, 628-654DOI: 10.1039/D4RA07942F
[3]. Nur-E-Alam M., Islam Md S., Abedin T., Islam M.A., Kar Yap B., Kiong T.S., Das N., Md R. Rahman, Khandaker M.U. Current scenario and future trends on stability issues of perovskite solar cells: A mini review. Current Opinion in Colloid & Interface Science. 2025,76. https://doi.org/10.1016/j.cocis.2025.101895.
[4]. Park S., Lee H.-J., Jang H.W. Harnessing ion migration in halide perovskites: Implication and applications. Solid State Ionics. 2025, 422, 2025, 116816. https://doi.org/10.1016/j.ssi.2025.116816.
[5]. Ma T., Zhao X., Yang X., Yan J., Luo D., Li M., Li X., Chen Ch., Song H., Tang J. Inhibiting Ion Migration and Oxidation in Sn–Pb Perovskite by Multidentate Chelating Additive Strategy Advanced Functional Materials. 2025, 35, 4, 2412216 https://doi.org/10.1002/adfm.202412216
[6]. Cachafeiro M.A.T., Comi E.L., Shaji Sh.P., Narbey S., Jenatsch S., Knapp E., Tress W.Ion Migration in Mesoscopic Perovskite Solar Cells: Effects on Electroluminescence, Open Circuit Voltage, and Photovoltaic Quantum Efficiency. Adv. Energy Mater. 2025, 15, 2403850. https://doi.org/10.1002/aenm.202403850
[7]. Li M., Li H., Zhuang Q., He D., Liu B., Chen C., Zhang B., Pauporté T., Zang Z., Chen J. Stabilizing Perovskite Precursor by Synergy of Functional Groups for NiOx-Based Inverted Solar Cells with 23.5% Efficiency. Angew. Chem. Int. Ed. 2022, 61, e202206914. DOI: 10.1002/anie.202206914
[8]. Padture N.P. Trade-offs at the interface. Nat Energy. 202510, 153–154. https://doi.org/10.1038/s41560-024-01691-8
[9]. Hou Y., Li J., Yin R., Su X., Su Y., Qiao L., Zhang Zh.,. Liu Ch, Bai Y. The critical role of phase transition and composition regulation in inorganic perovskite electrocaloric materials. J. Mater. Chem. C, 2025. https://doi.org/10.1039/D4TC05060F Advance Article
[10]. Tang Y., Liu Y., Li M. Perspectives on various-temperature stability of p-i-n perovskite solar cells. Appl. Phys. Lett. 2025, 6, 126 (1), 010502. https://doi.org/10.1063/5.0245576
[11]. Zheng X., Yang Sh., Zhu J., Liu R., Li L., et.al. Suppressing phase segregation and nonradiative losses by a multifunctional cross-linker for high-performance all-perovskite tandem solar cells. Energy Environ. Sci., 2025
[12]. Nurgaliev I.N., Marasulov M.B. Degradation mechanisms of perovskite solar cells: a review// Uzbekistan Journal of Polymers Vol. 3. Issue 2,2024. P.5-20
[13]. Nurgaliev I.N., Marasulov M.B., Ashurov N.R. Density Functional Theory and Molecular Dynamics Study of the Cation Substitution Effect on the Structure of Halide Perovskites. Journal Structural Chemistry. 2024, 65, 451–463. https://doi.org/10.1134/S002247662403003X
[14]. Nurgaliev I.N., Marasulov M.B., Ashurov N.R. The Role of Specific Interactions in the Formation of Perovskite Structures. Appl. Sol. Energy. 2023, 59, 612–620 (). https://doi.org/10.3103/S0003701X23601746
[15]. Mannodi-Kanakkithodi A. A guide to discovering next-generation semiconductor materials using atomistic simulations and machine learning, Computational Materials Science. 2024, 243, 113108. https://doi.org/10.1016/j.commatsci.2024.113108.
[16]. Sowmya K B, Bhavitha K R. Strategic DFT Implementation and Verification of Next–Gen Electronics Using ATPG Simulation," 2024 8th International Conference on Computational System and Information Technology for Sustainable Solutions (CSITSS), Bengaluru, India, 2024, 1-6. doi: 10.1109/CSITSS64042.2024.10817045.
[17]. Conesa J.C. Computing with DFT Band Offsets at Semiconductor Interfaces: A Comparison of Two Methods. Nanomaterials. 2021, 11, 1581. https://doi.org/10.3390/nano11061581
[18]. Dong B., Wei M., Li Y. et al. Self-assembled bilayer for perovskite solar cells with improved tolerance against thermal stresses. Nat. Energy. 2025. https://doi.org/10.1038/s41560-024-01689-2
[19]. Tian X., Stranks S.D., Huang J. et. al. Perspectives for sustainability analysis of scalable perovskite photovoltaics (Perspective) Energy Environ. Sci., 2025, 18, 194-213. DOI: 10.1039/D4EE03956D
[20]. Hossain M.I., Chelvanathan P., Aissa B. et al. Enhanced perovskite solar cells performance with TiOx and SnOx thin films as electron transport layers. Sci Rep. 2025, 15, 7709. https://doi.org/10.1038/s41598-024-83600-3
[21]. Gallant B.M., Holzhey P., Smith J.A. et al. A green solvent enables precursor phase engineering of stable formamidinium lead triiodide perovskite solar cells. Nat. Commun. 202415, 10110. https://doi.org/10.1038/s41467-024-54113-4
[22]. X. Guo, Zh.Jia, Sh. Liu, et. al. Stabilizing efficient wide-bandgap perovskite in perovskite-organic tandem solar cells. Joule. 2024, 8, 9, 2554-2569. https://doi.org/10.1016/j.joule.2024.06.009.
[23]. Lim E.L., Hagfeldt A., Bi D. Toward high efficient and stable Sn2+ and mixed Pb2+/Sn2+ based halide perovskite solar cells through device engineering. Energy & Environmental Science. 2021, 14, (6). DOI: 10.1039/D0EE03368E
[24]. Song Zh., Watthage S., Phillips A., Heben M. Pathways toward high-performance perovskite solar cells: Review of recent advances in organo-metal halide perovskites for photovoltaic applications. Journal of Photonics for Energy. 2016, 6, (2), 022001. DOI: 10.1117/1.JPE.6.022001

[25]. Haruyama J., Sodeyama K., Han L., Tateyama Y. First-Principles Study of Ion Diffusion in Perovskite Solar Cell Sensitizers. Journal of the American Chemical Society. J. Am. Chem. Soc. 2015, 137, 32, 10048–10051. https://doi.org/10.1021/jacs.5b03615

[26]. Miah Md. H., Khandaker M.U., Rahman Md.B., Nur-E-Alamd M., Islam M.A. Band gap tuning of perovskite solar cells for enhancing the efficiency and stability: issues and prospects. RSC Adv. 2024, 14, 15876-15906. DOI: 10.1039/D4RA01640H

[27]. Motta C., El-Mellouhi F., Kais S., Tabet N., Alharbi F., Sanvito S. Revealing the role of organic cations in hybrid halide perovskite $CH_3NH_3PbI_3$. Nat. Commu., 2015, 6, 7026.